Biophysical Journal, Volume *118*

Supplemental Information

Ligand Entry into Fatty Acid Binding Protein via Local Unfolding Instead of Gap Widening

Tianshu Xiao, Yimei Lu, Jing-song Fan, and Daiwen Yang

Table S1. Structural statistics for the final 20 conformers of hIFABP V60C/Y70C variant [a]

Distance restraints	
Intra-residue (i-j = 0)	383
Sequential ($\|i$-$j\|$ = 1)	427
Medium range ($2 \leq \|i$-$j\| \leq 4$)	113
Long range ($\|i$-$j\| \geq 5$)	354
Hydrogen bond	124
Total	1401
Dihedral angle restraints	
ϕ	115
ψ	115
Average rmsd to the mean structure (Å)[b]	
Backbone atoms	0.69 ± 0.13
Heavy atoms	1.53 ± 0.14
ϕ/ψ space[c]	
Most favored region (%)	72.5
Additionally allowed region (%)	22.9
Generously allowed region (%)	2.6
Disallowed region (%)	2.1
rmsd from covalent geometry	
Bonds (Å)	0.003 ± 0.000
Angles (deg.)	0.337 ± 0.011
Impropers (deg.)	0.291 ± 0.015
rmsd from experimental restraints	
NOEs (Å)	0.043 ± 0.000
Dihedral angles (deg.)	0.809 ± 0.019

[a] Selected from 100 calculated conformers according to overall energy.
[b] Calculated with MOLMOL over the structure region (3-131).
[c] Calculated with PROCHECK-NMR.

Table S2. ^{15}N chemical shifts of major native state (N), minor states (I_1, I_2, and I_3), and unfolded state (U).

Residue	N (ppm)	I_1 (ppm)	I_2 (ppm)	I_3 (ppm)	U (ppm)[a]	Structure
F2	114.19	116.23	111.65	117.18	119.272	
D3	119.04	118.29	118.28	120.40	121.971	
S4	120.18	117.41	122.68	115.04	116.534	
T5	115.69	114.06	115.22	116.11	116.443	
W6	128.15	125.87	129.14	122.18	122.706	
K7	122.87	121.02	123.5	123.88	123.208	βA
V8	127.24	126.36	126.41	126.29	121.446	
D9	128.13	127.41	128.72	128.69	124.144	
R10	112.89	n	n	n	122.72	
S11	113.57	112.89	112.65	114.26	117.18	
E12	122.32	122.91	121.06	121.59	122.652	
N13	-	-	-	-	118.90	
Y14	121.22	120.30	121.75	119.57	114.42	
D15	118.32	n	n	n	121.98	
K16	120.10	119.45	120.76	119.39	121.46	
F17	121.43	n	n	n	121.28	
M18	118.16	n	n	n	122.32	α1
E19	119.96	n	n	n	121.58	
K20	122.67	n	n	n	122.31	
M21	115.78	n	n	n	121.57	
G22	108.17	-	-	-	110.30	
V23	121.16	120.54	121.40	120.08	120.15	
N24	125.93	125.13	127.38	124.43	122.83	
I25	121.29	120.60	122.68	120.45	122.34	
V26	121.82	121.33	120.24	122.89	124.51	
K27	120.08	119.67	119.21	123.49	125.55	
R28	119.66	120.15	119.12	120.63	123.29	
K29	119.81	-	-	-	122.68	α2
L30	119.83	120.26	119.18	122.92	123.20	
A31	121.05	121.57	120.67	123.90	124.37	
A32	118.77	118.00	119.63	122.62	123.01	
H33	116.89	116.37	115.56	118.76	118.16	
D34	119.81	119.18	120.89	120.63	121.17	
N35	119.84	118.83	120.98	118.86	119.00	
L36	120.67	120.28	121.27	121.87	122.22	
K37	125.18	124.14	128.3	120.75	121.77	
L38	126.16	-	-	-	123.07	
I40	127.66	128.96	129.4	122.92	123.65	βB
T41	121.56	120.48	122.64	118.13	118.73	
Q42	127.50	126.50	126.28	122.59	122.94	
E43	128.06	127.53	127.76	122.12	122.12	
G44	117.60	-	-	-	109.12	
N45	125.20	-	-	-	118.44	

K46	120.61	n	n	n	121.69	
F47	126.15	-	-	-	121.55	
T48	115.67	116.68	119.10	115.28	116.85	
V49	126.65	126.17	127.25	122.76	123.32	βC
K50	128.95	127.63	123.65	125.14	125.60	
E51	125.40	126.52	128.64	122.11	123.11	
S52	120.16	121.03	121.25	116.35	117.39	
S53	120.83	119.88	115.25	117.82	118.08	
A54	-	-	-	-	125.75	
F55	113.76	112.99	116.18	117.38	119.26	
R56	116.65	116.01	117.86	118.82	122.56	
N57	-	-	-	-	120.17	
I58	121.51	120.27	117.73	120.42	122.02	
E59	126.04	125.38	125.65	124.48	124.70	βD
C60	122.73	122.43	122.95	116.17	119.76	
V61	126.06	126.07	124.20	121.11	121.57	
F62	121.27	121.95	123.10	126.83	124.27	
E63	119.90	120.50	120.32	119.40	123.32	
L64	124.63	125.40	123.64	121.65	122.95	
G65	108.90	108.42	110.17	109.84	109.46	
V66	122.31	121.72	121.78	119.30	120.42	
T67	129.49	128.61	128.47	130.04	118.68	
F68	126.16	-	-	-	123.37	
N69	117.55	117.89	116.68	115.90	120.44	βE
C70	119.23	118.79	119.5	116.34	118.03	
N71	122.77	121.88	123.71	116.81	119.48	
L72	118.94	119.91	121.2	118.24	122.41	
A73	-	-	-	-	124.33	
D74	112.86	113.95	113.96	112	119.15	
G75	107.95	107.77	108.71	107.51	109.27	
T76	119.81	-	-	-	114.42	
E77	128.91	128.46	128.60	129.35	123.32	
L78	125.01	124.37	125.37	126.21	123.05	
R79	121.03	121.80	120.67	119.46	121.62	
G80	116.16	n	n	n	109.96	βF
T81	107.53	107.95	107.81	106.86	114.35	
W82	119.59	118.81	120.79	123.14	122.84	
S83	115.75	n	n	n	117.28	
L84	126.00	n	n	n	109.12	
E85	128.33	127.80	129.09	127.67	121.17	
G86	117.60	-	-	-	109.14	
N87	123.29	-	-	-	118.44	
K88	118.57	117.90	118.82	119.30	121.66	
L89	123.30	122.40	121.42	124.23	123.20	
I90	125.44	n	n	n	121.51	
G91	122.01	122.43	122.30	120.41	112.62	βG
K92	128.43	127.81	128.06	129.14	121.09	
F93	121.41	120.82	121.9	122.61	121.34	

K94	119.29	n	n	n	123.35	
R95	121.88	n	n	n	122.52	
T96	115.59	n	n	n	116.01	
D97	120.72	n	n	n	122.52	
N98	116.85	n	n	n	119.18	
G99	108.17	-	-	-	108.68	
N100	119.59	n	n	n	118.46	
E101	120.42	n	n	n	121.12	
L102	124.73	124.38	125.29	124.34	122.73	
N103	124.73	n	n	n	119.32	
T104	118.19	117.74	118.94	117.27	115.25	βH
V105	127.09	n	n	n	123.28	
R106	124.62	n	n	n	125.28	
E107	122.14	123.59	121.62	121.21	122.96	
I108	125.20	-	-	-	122.19	
I109	130.33	n	n	n	124.96	
G110	119.29	n	n	n	112.68	
D111	125.20	-	-	-	119.88	
E112	118.83	118.83	119.19	118.09	121.22	
L113	123.86	n	n	n	123.02	
V114	128.32	n	n	n	121.05	
Q115	130.80	131.27	130.43	131.20	124.32	βI
T116	121.76	120.66	120.29	117.75	116.13	
Y117	126.00	126.90	125.29	124.75	122.54	
V118	120.22	119.75	120.83	121.35	122.36	
Y119	128.37	n	n	n	123.96	
E120	126.31	n	n	n	123.73	
G121	102.73	n	n	n	110.35	
V122	123.63	n	n	n	120.47	
E123	126.58	n	n	n	124.91	
A124	126.15	-	-	-	125.81	
K125	117.07	117.54	117.67	116.29	120.54	
R126	121.04	121.82	121.78	120.60	122.31	βJ
I127	123.65	124.18	122.93	122.86	122.23	
F128	126.92	n	n	n	124.10	
K129	118.71	119.87	118.42	118.20	123.41	
K130	124.00	125.42	123.42	122.85	122.18	
D131	130.09	129.34	129.3	130.73	127.02	

-: Due to peak overlap or weak signal, the data are not available.
n: No obvious relaxation dispersion (R_{ex} < 2 s^{-1}) and no minor CEST dips, implying that the chemical shifts of the minor states are similar to those of state N.
[a:] The chemical shifts in the unfolded state were predicted using an online predictor tool (http://desimone.bio.ic.ac.uk/prosecco/, Sanz-Hernández M & De Simone A, J Biomol NMR, 2017, 69:147-156).

Table S3. Amide hydrogen exchange rates (k_{obs}) and protection factors (PF)

Residue	k_{obs} (s^{-1})[a],pH 7.0	k_{rc} (s^{-1})[b],pH 7.0	k_{obs} (s^{-1}),pH 7.2	PF (k_{rc}/k_{obs})[c]	Structure
F2	0.4±0.1	19.6	0.7±0.1	49	
D3	0.5±0.1	19.8	0.8±0.1	40	
S4	0.8±0.2	53.1	1.2±0.1	66	
T5	1.3±0.2	57.9	2.1±0.1	44	
W6	$(7.7\pm0.3)\times10^{-4}$	21.0	$(1.2\pm0.1)\times10^{-3}$	2.7×10^{4}	
K7	$(8.2\pm0.4)\times10^{-4}$	24.1	$(1.2\pm0.1)\times10^{-3}$	2.9×10^{4}	βA
V8	$(7.6\pm0.6)\times10^{-3}$	9.0	$(8.6\pm0.7)\times10^{-3}$	1.2×10^{3}	
D9	$(8.6\pm0.4)\times10^{-4}$	12.5	$(1.4\pm0.1)\times10^{-3}$	1.4×10^{4}	
R10	$(1.2\pm0.1)\times10^{-3}$	27.2	$(1.7\pm0.1)\times10^{-3}$	2.3×10^{4}	
S11	3.4±0.2	133	5.4±0.2	39	
E12	$(8.0\pm1.3)\times10^{-3}$	21.1	$(1.2\pm0.2)\times10^{-2}$	2.6×10^{3}	
N13	-	74.9	-	-	
Y14	1.0±0.2	38.3	1.5±0.2	38	
D15	12.9±0.7	19.3	22.7±1.0	1.5	
K16	0.8±0.1	20.7	1.3±0.1	26	
F17	$(5.0\pm0.1)\times10^{-4}$	25.9	$(7.4\pm0.1)\times10^{-4}$	5.1×10^{4}	
M18	$(4.6\pm0.1)\times10^{-4}$	38.3	$(6.9\pm0.1)\times10^{-4}$	8.2×10^{4}	α1
E19	$(6.1\pm0.1)\times10^{-4}$	13.7	$(8.5\pm0.1)\times10^{-4}$	2.2×10^{4}	
K20	$(9.4\pm0.2)\times10^{-4}$	22.1	$(1.4\pm0.1)\times10^{-3}$	2.3×10^{4}	
M21	$(1.1\pm0.1)\times10^{-3}$	43.9	$(1.4\pm0.1)\times10^{-3}$	4.0×10^{4}	
G22	0.2±0.1	81.8	0.2±0.1	409	
V23	0.2±0.1	10.1	0.3±0.1	50	
N24	10.6±0.4	76.4	17.6±0.4	7	
I25	5.4±0.3	13.3	8.3±0.1	2.5	
V26	1.3±0.1	4.0	2.2±0.1	3	
K27	5.5±0.2	22.5	8.9±0.2	4	
R28	7.7±0.6	54.1	12.4±0.4	7	
K29	-	51.6	-	-	α2
L30	3.6±0.2	11.8	5.9±0.2	3.3	
A31	5.9±0.3	21.0	9.8±0.4	3.6	
A32	8.3±0.4	34.1	13.5±0.5	4.1	
H33	11.9±0.6	57.1	18.3±0.8	4.8	
D34	6.9±0.3	42.1	10.3±0.4	6.1	
N35	9.0±0.5	70.0	13.7±0.5	7.8	
L36	0.5±0.1	18.7	0.8±0.1	37	
K37	0.2±0.1	19.2	0.2±0.1	96	
L38	-	11.8	-	-	
T39	0.3±0.1	17.9	0.4±0.1	60	βB
I40	0.3±0.1	10.1	0.5±0.1	34	
T41	1.4±0.2	17.1	2.0±0.1	12	
Q42	0.3±0.1	62.1	0.6±0.1	207	
E43	0.3±0.1	16.8	0.5±0.1	56	
G44	-	45.1	-	-	
N45	10.9±0.7	156	17.4±0.4	14	
K46	0.7±0.1	65.0	1.1±0.1	93	

F47	-	25.9	-	-	
T48	2.4±0.2	33.3	3.4±0.2	14	
V49	0.2±0.1	10.8	0.2±0.1	52	βC
K50	0.2±0.1	22.5	0.3±0.1	112	
E51	0.02-0.2	14.0	0.02-0.2	70-700	
S52	0.2±0.1	56.8	0.3±0.1	284	
S53	0.5±0.1	160	0.8±0.1	320	
A54	-	68.1	-	-	
F55	3.9±0.2	19.6	6.5±0.2	5.0	
R56	1.5±0.1	47.1	2.4±0.1	31	
N57	-	175	-	-	
I58	0.2±0.1	13.3	0.2±0.1	66	
E59	2.3±0.1	6.2	3.6±0.1	2.7	βD
C60	0.02-0.2	86.0	0.02-0.2	$430\text{-}4.3\times10^{3}$	
V61	0.02-0.2	19.6	0.02-0.2	98-980	
F62	$(7.1\pm0.1)\times10^{-4}$	14.2	$(1.1\pm0.1)\times10^{-3}$	2.0×10^{4}	
E63	$(3.2\pm0.2)\times10^{-3}$	12.2	$(4.8\pm0.4)\times10^{-3}$	3.8×10^{3}	
L64	$(3.8\pm0.3)\times10^{-3}$	6.4	$(5.3\pm0.4)\times10^{-3}$	1.7×10^{3}	
G65	$(5.3\pm0.5)\times10^{-3}$	39.2	$(1.4\pm0.4)\times10^{-2}$	7.4×10^{3}	
V66	$(6.4\pm0.1)\times10^{-4}$	10.1	$(1.0\pm0.1)\times10^{-3}$	1.6×10^{4}	
T67	9.9±0.5	21.0	16.9±0.5	2.1	
F68	$(7.1\pm0.7)\times10^{-3}$	31.1	$(7.3\pm0.8)\times10^{-3}$	4.4×10^{3}	
N69	0.2±0.1	121	0.4±0.1	605	βE
C70	$(9.4\pm2.3)\times10^{-3}$	253	0.02-0.2	2.7×10^{4}	
N71	5.9±0.3	304	9.1±0.1	52	
L72	$(4.5\pm0.4)\times10^{-3}$	18.7	$(6.8\pm0.5)\times10^{-3}$	4.2×10^{3}	
A73	-	21.0	-	-	
D74	7.8±0.3	17.2	12.7±0.4	2.2	
G75	2.2±0.2	42.2	3.7±0.1	19	
T76	2.5±0.1	42.9	3.1±0.1	17	
E77	0.4±0.1	16.8	0.6±0.1	42	
L78	$(9.9\pm0.4)\times10^{-4}$	6.4	$(1.5\pm0.1)\times10^{-3}$	6.5×10^{3}	
R79	$(6.2\pm0.1)\times10^{-5}$	25.3	$(1.2\pm0.1)\times10^{-4}$	4.1×10^{5}	
G80	$(1.3\pm0.1)\times10^{-3}$	105	$(1.8\pm0.1)\times10^{-3}$	7.8×10^{4}	βF
T81	$(6.2\pm0.1)\times10^{-5}$	42.9	$(1.3\pm0.1)\times10^{-4}$	7.0×10^{5}	
W82	$(5.0\pm0.3)\times10^{-5}$	21.0	$(1.1\pm0.1)\times10^{-4}$	4.2×10^{5}	
S83	$(5.8\pm0.2)\times10^{-5}$	62.1	$(1.2\pm0.1)\times10^{-4}$	1.1×10^{6}	
L84	0.7±0.1	17.9	1.0±0.1	26	
E85	$(6.8\pm0.9)\times10^{-3}$	6.5	$(1.5\pm0.1)\times10^{-3}$	956	
G86	-	45.1	-	-	
N87	8.5±0.4	156	13.2±0.4	18	
K88	$(1.8\pm0.1)\times10^{-3}$	65.0	$(2.4\pm0.1)\times10^{-3}$	3.6×10^{4}	
L89	$(2.9\pm0.1)\times10^{-5}$	11.8	$(7.0\pm0.2)\times10^{-5}$	4.1×10^{5}	
I90	$(1.9\pm0.1)\times10^{-5}$	3.9	$(4.7\pm0.2)\times10^{-5}$	2.1×10^{5}	
G91	$(7.2\pm0.2)\times10^{-5}$	37.4	$(1.5\pm0.1)\times10^{-4}$	5.2×10^{5}	βG
K92	$(3.0\pm0.1)\times10^{-4}$	46.0	$(5.0\pm0.1)\times10^{-4}$	1.6×10^{5}	
F93	$(1.5\pm0.1)\times10^{-4}$	25.9	$(2.8\pm0.1)\times10^{-4}$	1.8×10^{5}	
K94	$(4.5\pm0.1)\times10^{-4}$	35.7	$(7.0\pm0.1)\times10^{-4}$	8.0×10^{4}	

R95	$(7.3\pm0.6)\times10^{-4}$	54.1	$(1.8\pm0.6)\times10^{-3}$	7.4×10^{4}	
T96	0.7±0.1	48.2	1.2±0.1	69	
D97	0.3±0.1	27.3	0.4±0.1	91	
N98	0.5±0.1	70.0	0.9±0.1	140	
G99	0.3±0.1	133	0.4±0.1	443	
N100	$(5.6\pm0.3)\times10^{-3}$	156	$(1.0\pm0.1)\times10^{-2}$	2.8×10^{4}	
E101	$(1.6\pm0.6)\times10^{-2}$	22.1	0.02-0.2	1.4×10^{3}	
L102	$(3.6\pm0.1)\times10^{-4}$	6.4	$(5.9\pm0.1)\times10^{-4}$	1.8×10^{4}	
N103	$(8.8\pm0.2)\times10^{-4}$	65.0	$(1.2\pm0.1)\times10^{-3}$	7.4×10^{4}	
T104	$(9.8\pm0.2)\times10^{-4}$	60.7	$(1.3\pm0.1)\times10^{-3}$	6.2×10^{4}	
V105	$(4.3\pm0.1)\times10^{-4}$	10.8	$(6.1\pm0.1)\times10^{-4}$	2.5×10^{4}	βH
R106	$(5.2\pm0.1)\times10^{-4}$	29.7	$(6.9\pm0.1)\times10^{-4}$	5.7×10^{4}	
E107	$(5.5\pm0.2)\times10^{-4}$	17.6	$(6.8\pm0.2)\times10^{-4}$	3.2×10^{4}	
I108	$(2.0\pm0.1)\times10^{-3}$	4.5	$(2.5\pm0.1)\times10^{-3}$	2.3×10^{3}	
I109	$(3.5\pm0.1)\times10^{-4}$	3.7	$(5.5\pm0.1)\times10^{-4}$	1.1×10^{4}	
G110	6.4±0.1	37.4	9.4±0.3	5.8	
D111	1.2±0.1	25.5	1.7±0.1	21	
E112	$(3.3\pm0.1)\times10^{-4}$	7.0	$(5.3\pm0.1)\times10^{-4}$	2.1×10^{4}	
L113	$(2.1\pm0.1)\times10^{-4}$	6.4	$(3.3\pm0.1)\times10^{-4}$	3.1×10^{4}	
V114	$(6.2\pm0.2)\times10^{-5}$	4.2	$(1.4\pm0.1)\times10^{-4}$	6.7×10^{4}	
Q115	$(3.5\pm0.1)\times10^{-4}$	28.4	$(5.4\pm0.1)\times10^{-4}$	8.2×10^{4}	βI
T116	$(5.1\pm0.2)\times10^{-4}$	46.0	$(8.0\pm0.2)\times10^{-4}$	9.0×10^{4}	
Y117	$(1.8\pm0.1)\times10^{-4}$	29.0	$(3.2\pm0.1)\times10^{-4}$	1.6×10^{5}	
V118	$(1.1\pm0.1)\times10^{-4}$	7.6	$(2.0\pm0.1)\times10^{-4}$	6.9×10^{4}	
Y119	$(1.2\pm0.1)\times10^{-4}$	13.3	$(2.2\pm0.1)\times10^{-4}$	1.1×10^{5}	
E120	0.3±0.1	11.9	0.4±0.1	40	
G121	0.02-0.2	45.1	0.2±0.1	$226\text{-}2.3\times10^{3}$	
V122	$(6.2\pm0.1)\times10^{-4}$	10.1	$(9.2\pm0.1)\times10^{-4}$	1.6×10^{4}	
E123	$(6.1\pm0.4)\times10^{-3}$	7.7	$(7.1\pm0.5)\times10^{-3}$	1.3×10^{3}	
A124	$(7.7\pm0.2)\times10^{-4}$	24.2	$(9.2\pm0.2)\times10^{-4}$	3.1×10^{4}	
K125	$(1.1\pm0.1)\times10^{-3}$	31.1	$(1.5\pm0.1)\times10^{-3}$	2.8×10^{4}	
R126	$(1.1\pm0.1)\times10^{-3}$	54.1	$(1.4\pm0.1)\times10^{-3}$	4.9×10^{4}	βJ
I127	$(4.8\pm0.2)\times10^{-4}$	10.5	$(6.9\pm0.2)\times10^{-4}$	2.2×10^{4}	
F128	$(8.4\pm0.3)\times10^{-4}$	11.6	$(1.1\pm0.1)\times10^{-3}$	1.4×10^{4}	
K129	$(9.8\pm0.5)\times10^{-4}$	35.7	$(1.3\pm0.1)\times10^{-3}$	3.6×10^{4}	
K130	$(4.3\pm0.2)\times10^{-3}$	41.0	$(5.6\pm0.2)\times10^{-3}$	9.5×10^{3}	
D131	$(3.4\pm0.1)\times10^{-3}$	0.4	$(3.8\pm0.1)\times10^{-3}$	118	

-: due to peak overlap or weak signal, the data are not available.
[a]: For the exchange rates larger than 0.2 s^{-1}, they were measured by the amide hydrogen exchange method in 95% H2O and 5% D2O. For the rates smaller than 0.02 s^{-1}, they were measured by the H-D exchange method.
[b]: krc was predicted using an online software tool (https://protocol.fccc.edu/research/labs/roder/sphere/sphere.html, Bai, Milne, Mayne & Englander, *Proteins* 17: 75-86 (1993). The reference data are from alanine in oligo-peptide.
[c]: Protection Factor (PF) was calculated from the data at pH 7.0.

Table S4. Comparison of fitting results derived from the stopped-flow data at low oleic acid concentrations using the bi- and mono-exponential models.

Oleic acid concentration (μM)	Bi-exponential model			Mono-exponential model		F-statistic
	k_1 [a]	k_2 [b]	χ^2 [c]	k_1 [d]	χ^2	
10.0	426	16	1.698	394	1.998	87.9
12.5	561	25	3.604	471	5.405	248.2
15.0	716	30	1.718	564	3.449	500.8
17.5	807	29	1.964	710	2.505	136.7
25.0	-	-	-	956 [e]	2.010 [e]	-
35.0	-	-	-	1010 [e]	2.312 [e]	-

[a]: apparent association rate for the fast step.
[b]: apparent association rate for the slow step.
[c]: sum of squared residuals.
[d]: apparent association rate for a one-step association.
[e]: the results were obtained by fitting the data points within a mixing time of 10 ms.

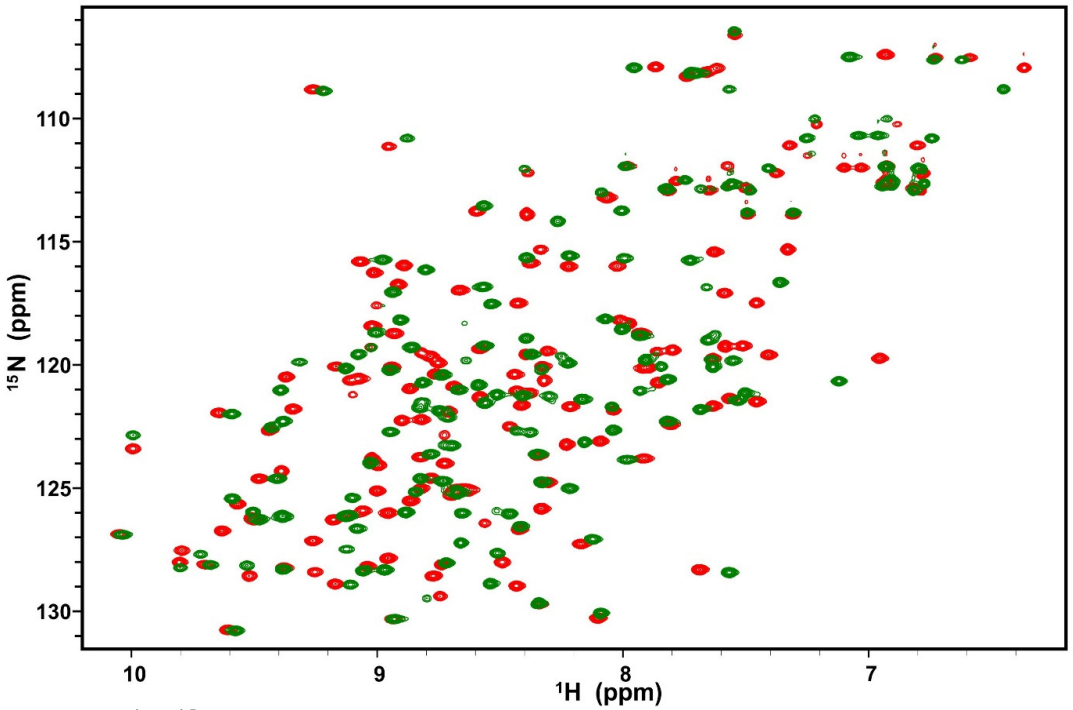

Figure S1. ^{1}H-^{15}N HSQC spectra of reduced (red, in presence of DTT) and oxidized hIFABP V60C/Y70C variant (green, in the absence of DTT).

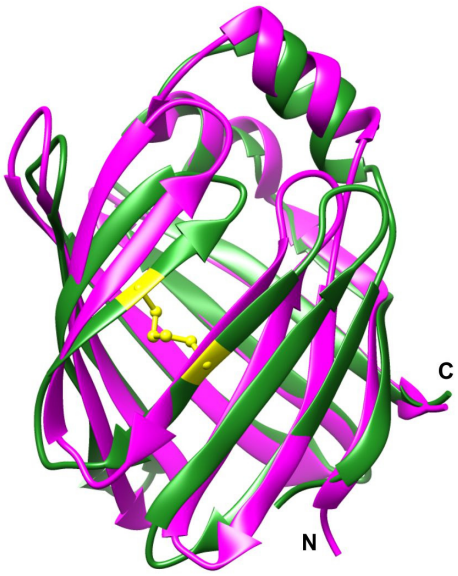

Figure S2. Struture comparison of WT hIFABP (pink) and its variant (dark green).

The disulfide linkage is displayed in sticks and balls (yellow).

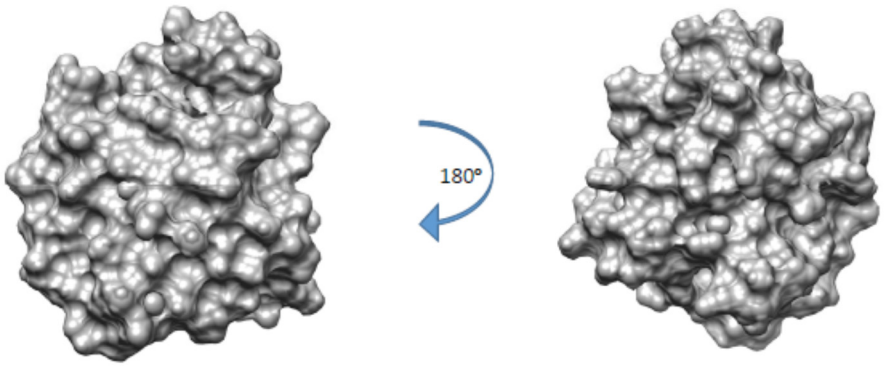

Figure S3. Surface representation of gap-closed hIFABP variant. The structure in the left panel has the same orientation as the structure in Figure S2.

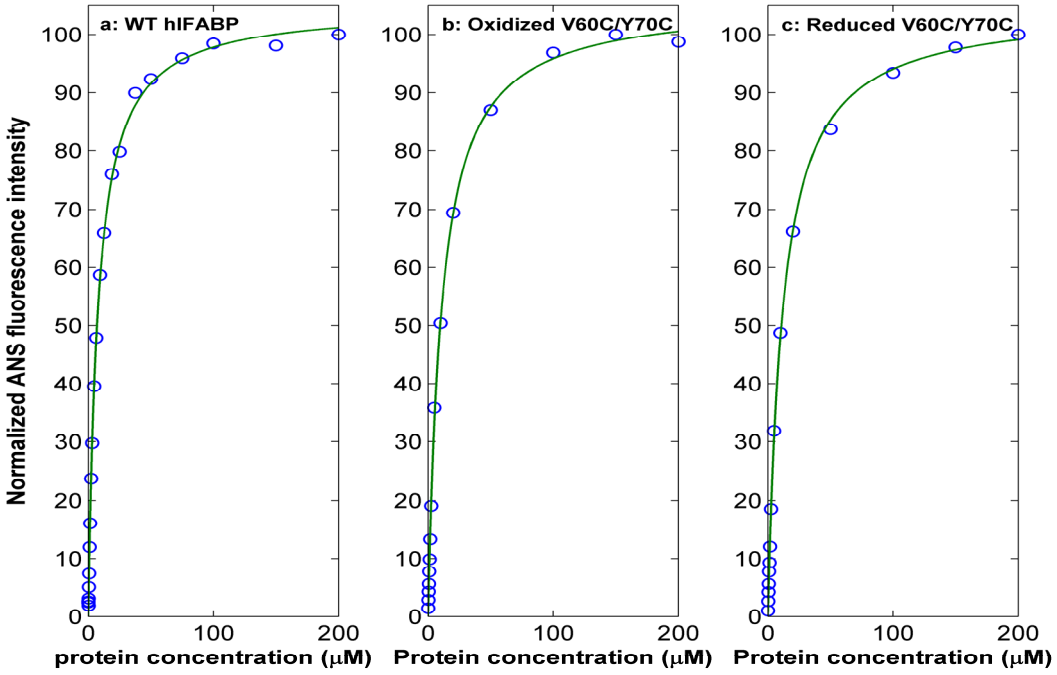

Figure S4. Dependence of ANS fluorescence intensities on concentrations of WT hIFABP (a) and oxidized (b) and reduced (c) V60C/Y70C variants. Experimental data are indicated by 'o', while the best fits are shown in solid lines.

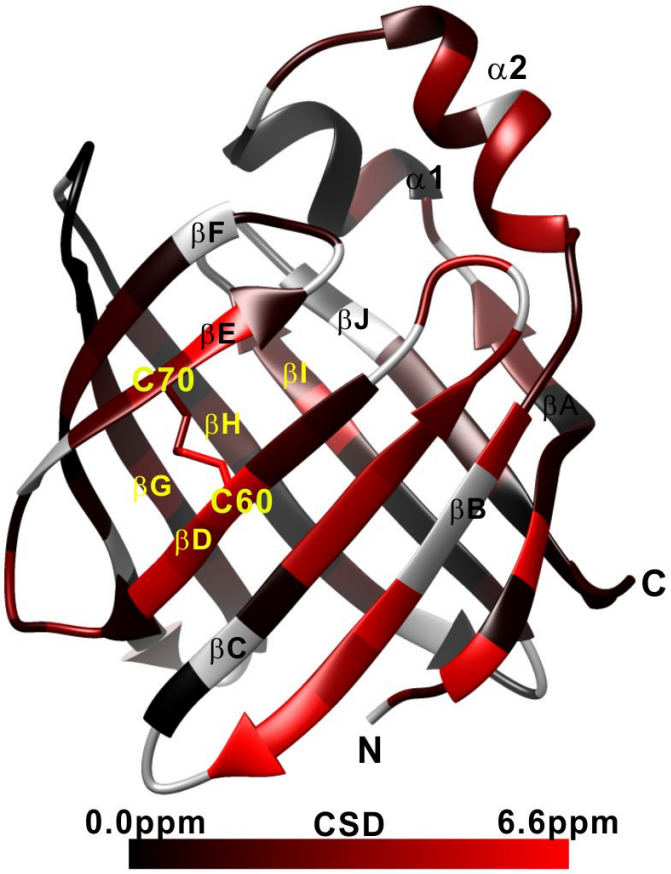

Figure S5. ^{15}N chemical shift differences (CSD) of states N and I3 mapped onto the 3D structure of the gap-closed mutant. The differences are color-coded. The residues with unavailable data are indicated in gray.

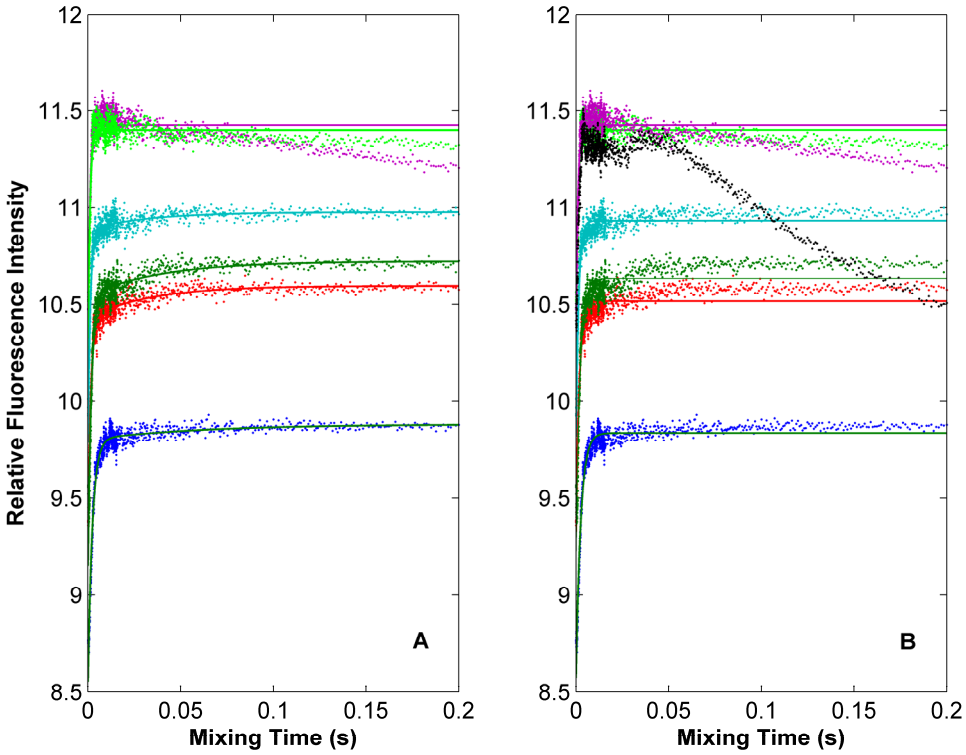

Figure S6. Stopped-flow traces (dots) of the hIFABP V60C/Y70C variant recorded at 20 °C, and their best fits (solid lines) to a double exponential function (A, at concentrations smaller than 25 µM) and single exponential function (A, at concentrations of 25 and 35 µM, and B). The traces were recorded at final oleic acid concentrations of 10 µM (blue), 12.5 µM (red), 15 µM (dark green), 17.5 µM (cyan), 25 µM (green), 35 µM (purple), and 50 µM (black).